ChemPubSoc Europe

DOI: 10.1002/celc.201801517

CHEMELECTROCHEM Articles

Effect of Organic Solvents on the Electrochemical Performance of Sodium-Ion Hybrid Capacitors

Myung-Soo Park,[a] Ganesh Kumar Veerasubramani,[a] Ranjith Thangavel,[b] Yun-Sung Lee,[b] and Dong-Won Kim*[a]

A comparative study on the ionic conductivity of carbonate- and ether-based electrolytes was performed, which showed that the ionic conductivity was strongly affected by the dielectric constant of the organic solvent. The relationship between the physicochemical properties of a liquid electrolyte and the cycling performance of sodium-ion hybrid capacitors (SICs) was assessed by comparing the electrochemical characteristics of SICs assembled with a negative activated carbon electrode and a positive $Na_3V_2(PO_4)_3$ electrode. Cyclic voltammetry, leakage current measurements, and electrochemical impedance spectroscopy results demonstrated that the good cycling performance of SICs with carbonate-based electrolytes can be ascribed to their superior electrochemical stability, large amounts of free ions, and favorable electrochemical reaction kinetics. An SIC employing an electrolyte consisting of 1.0 M $NaClO_4$ in ethylene carbonate/propylene carbonate exhibited a good rate capability and delivered a high initial discharge capacity of 98.7 mAh g^{-1} with a capacity retention of 90.8% after 1000 cycles at a constant current density of 500 mA g^{-1}.

1. Introduction

The development of green renewable energy sources and energy storage systems has become an important issue due to the limited amounts of fossil fuels and increasing demand for efficient energy management. Among a variety of energy storage devices, lithium-ion batteries (LIBs) have been a leading power source for portable electronic devices, electric vehicles and large-scale energy storage systems due to their long cycle life and high energy density.[1] However, the rising price of lithium sources has become a significant concern; it is arising from the increasing market demand for LIBs and the limited lithium resources.[2] In this respect, energy storage devices based on sodium-ion (sodium-ion batteries or sodium-ion hybrid capacitors) have received great attention because they can resolve the current cost issues of LIBs thanks to the highly abundant sodium resources.[2b–c,3] Furthermore, similar synthetic strategies and characterization techniques utilized for materials in LIBs can be used in their sodium counterparts due to the close relationship between these two alkali metals.[4] Recently, sodium-ion hybrid capacitors (SICs) have been actively studied because of their high-power density, excellent cycle life and relatively high energy density.[5] The SICs usually consist of non-faradaic (carbonaceous materials) and faradaic (intercalation materials) electrodes with an Na^+ ion-conducting electrolyte. High power density and energy density of SICs can be achieved simultaneously via the surface adsorption/desorption of ions on the non-faradaic electrode and redox reactions at the faradaic electrode.[6] Many electrode materials, including $Na_3V_2(PO_4)_3$, $NaTi_2(PO_4)_3$, $Na_2Ti_2O_4(OH)_2$, Nb_2O_5, MXenes and biomass-derived activated carbon have been investigated for use in SICs because of their high discharge capacity, good rate capability and excellent cycling stability.[5a–b,7] Although a lot of electrode materials for SICs have been actively investigated so far, there are few reports on systematic studies of Na^+ ion-conducting electrolytes for SICs, except for few papers on sodium-ion batteries.[8]

In this study, we investigated the effect of electrolyte solvent on the electrochemical performance of SICs. We chose three carbonate-based solvents (ethylene carbonate (EC), diethyl carbonate (DEC) and propylene carbonate (PC)) and three ether-based solvents (1,2-dimethoxyethane (DME), diethylene glycol dimethyl ether (DEGDME) and tetraethylene glycol dimethyl ether (TEGDME)), to address the relationships between the physicochemical properties of the electrolytes (ionic conductivity, degree of salt dissociation, viscosity, electrochemical stability and reaction kinetics) and the electrochemical performance of SICs. $NaClO_4$ was chosen as a salt in the electrolyte since it is highly dissociated in organic solvents. A high degree of $NaClO_4$ dissociation into free ions is advantageous for achieving high capacity in SICs. Electrolytes employing different types of organic solvents and $NaClO_4$ were prepared and applied to SICs consisting of an activated carbon (AC) negative electrode and a $Na_3V_2(PO_4)_3$ (NVP) positive electrode. $Na_3V_2(PO_4)_3$ was used as an active material in the positive electrode because of its super-ionic conductive structure (NASICON), which facilitates faster Na-ion diffusion in the electrode.[9] Our results demonstrate that SICs assembled with carbonate-based electrolytes exhibit higher discharge capacity, superior rate capability and better cycling stability

[a] M.-S. Park, Dr. G. K. Veerasubramani, Prof. D.-W. Kim
Department of Chemical Engineering
Hanyang University
Seoul 04763, Republic of Korea
E-mail: dongwonkim@hanyang.ac.kr
[b] R. Thangavel, Prof. Y.-S. Lee
Faculty of Applied Chemical Engineering
Chonnam National University
Gwangju 61186, Republic of Korea

Supporting information for this article is available on the WWW under https://doi.org/10.1002/celc.201801517

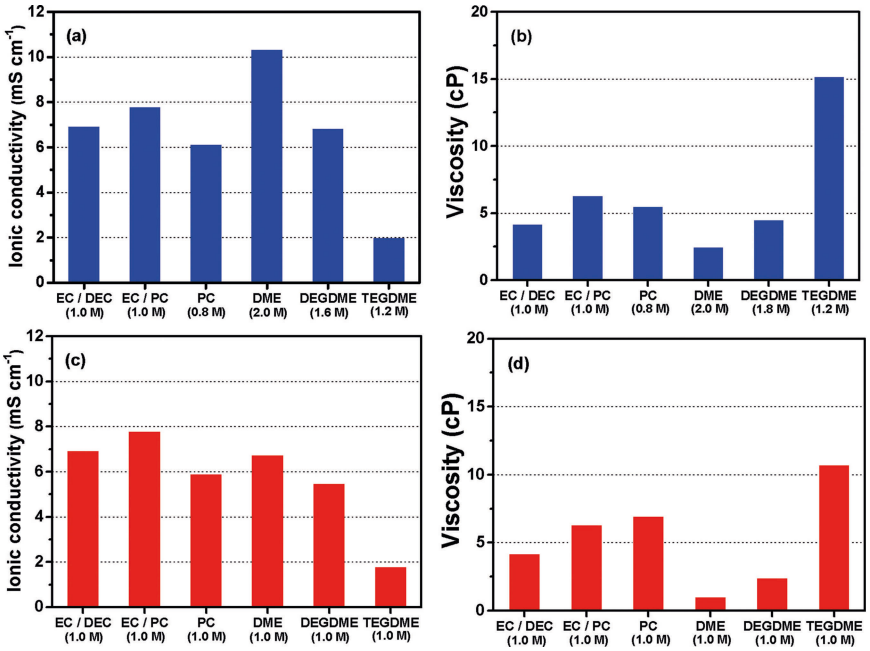

Figure 1. a) Ionic conductivities and b) viscosities of optimized liquid electrolytes dissolving $NaClO_4$ at 25 °C. c) Ionic conductivities and d) viscosities of liquid electrolytes dissolving 1.0 M $NaClO_4$ at 25 °C.

than those employing ether-based electrolytes because of their high electrochemical stability, large amounts of free ions and favorable charge/discharge kinetics.

2. Results and Discussion

Various carbonate- and ether-based solvents were chosen to investigate the effect of organic solvent on the electrochemical properties of electrolytes. Their molecular structure and physicochemical characteristics are summarized in Table S1. It can be seen from the data in the table that cyclic carbonates such as EC and PC have a high dielectric constant and high viscosity due to large mutual interactions between polar solvent molecules. In contrast, DEC corresponding to linear carbonate has a low dielectric constant and low viscosity. In this study, EC/DEC (50/50 by volume), EC/PC (50/50 by volume) and PC were considered as the carbonate solvent. DME, DEGDME and TEGDME were used as the ether solvent to investigate the effect of their physicochemical properties on the cycling performance of SICs. Ether solvents have similar dielectric constant, but quite different viscosities based on the number of ethylene oxide (EO, $-CH_2CH_2O-$) units. In these electrolytes, $NaClO_4$ was used as a salt because it has higher solubility in the organic solvent than $NaPF_6$, as demonstrated in Figure S1.

Figure S2 presents the ionic conductivities and viscosities of different electrolytes as a function of $NaClO_4$ concentration at room temperature. Ionic conductivity was increased with salt concentration and reached a maximum value at the optimum $NaClO_4$ concentration. This result can be attributed to two conflicting effects on ionic conductivity. At low salt concentrations, there is a buildup of free ions with increasing salt concentration. However, both viscosity and ion aggregates increase with increasing salt concentration, which consequently decreases the ionic conductivity. From the salt concentration dependent ionic conductivity behavior, the optimum $NaClO_4$ concentration for achieving the highest ionic conductivity was determined for each electrolyte. Figure 1a and 1b show the ionic conductivities and viscosities of various electrolytes at optimized $NaClO_4$ concentrations. The salt concentration given in parentheses is an optimum concentration showing maximum ionic conductivity in Figure S2a. Among the carbonate-based electrolytes, the EC/PC electrolyte exhibited the highest ionic conductivity of 7.8 mS cm^{-1} at 1.0 M $NaClO_4$. This result indicates that the dielectric constant has a critical influence on ionic conductivity for the carbonate-based electrolytes. In the case of the ether-based electrolytes, the ionic conductivity followed the order of DME > DEGDME > TEGDME, which suggests that the viscosity has the most influence on ionic conductivity in these ether-based electrolytes. Interestingly, the optimum salt concentration was decreased with increasing number of EO unit, since the viscosity was increased with an increase in the length of the EO unit. Among the electrolytes investigated, the DME electrolyte showed the highest ionic conductivity of 10.3 mS cm^{-1} at 2.0 M $NaClO_4$. However, the EC/PC electrolyte exhibited the highest ionic conductivity when comparing the ionic conductivity at the same salt concentration (1.0 M $NaClO_4$), although it had a relatively a high viscosity, as depicted in Figure 1c and 1d. This was attributed to large amounts of free ions in the EC/PC electrolyte. This result suggests that the ionic conductivity of the electrolyte is more influenced by the number of free ions rather than ionic mobility in the electrolyte at the same salt concentration.

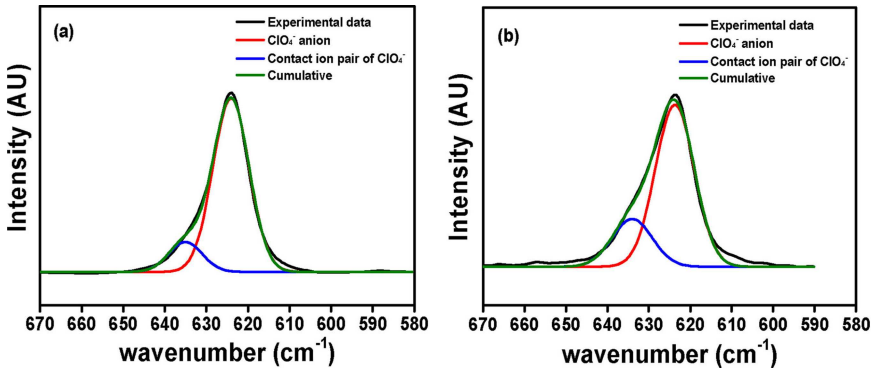

Figure 2. ATR-FTIR spectra of: a) 1.0 M $NaClO_4$-EC/PC and b) 1.0 M $NaClO_4$-DME in the wavenumber range: 580–670 cm^{-1}.

To understand the effect of the dielectric constant of the organic solvent on the number of free ions in the electrolyte, we investigated the dissociation behavior of $NaClO_4$ in different solvents at a salt concentration of 1.0 M by ATR-FTIR spectroscopy. The representative spectra of the 1.0 M $NaClO_4$-EC/PC and 1.0 M $NaClO_4$-DME electrolytes in the wavenumber range of 580 to 670 cm^{-1} are shown in Figure 2. The peak could be deconvoluted into two Gaussian peaks to analyze the relative degree of dissociation of $NaClO_4$. In the resolved spectra, the peaks at 623 and 635 cm^{-1} can be assigned to the dissociated ClO_4^- anion and the contact ion-pairs of ClO_4^- anions, respectively.[10] Using these deconvoluted peaks, the relative degree of salt dissociation in various electrolytes colud be calculated, and the results are summarized in Table 1.

Table 1. Relative degree of salt dissociation in the different electrolytes at 1.0 M concentration

Electrolyte	Dissociated anion [%]	Contact ion pairs [%]
1.0 M $NaClO_4$ in EC/DEC	82.1	17.9
1.0 M $NaClO_4$ in EC/PC	86.2	13.8
1.0 M $NaClO_4$ in PC	81.9	17.2
1.0 M $NaClO_4$ in DME	76.7	23.3
1.0 M $NaClO_4$ in DEGDME	78.1	21.9
1.0 M $NaClO_4$ in TEGDME	80.7	20.3

As expected, the 1.0 M $NaClO_4$-EC/PC electrolyte showed the highest degree of dissociation due to the highest dielectric constant of organic solvents. This is well consistent with the previous result that the highest ionic conductivity in EC/PC electrolyte at 1.0 M $NaClO_4$ can be attributed to the largest number of free ions. Clearly, the degree of salt dissociation was decreased with decreasing dielectric constant of the organic solvent. Accordingly, the DME electrolyte exhibited the lowest degree of salt dissociation. In addition, we estimated the relative degree of salt dissociation for various electrolytes at optimum $NaClO_4$ concentration, as given in Table S2. In ether-based electrolytes, the relative fraction of free ions was decreased with increasing $NaClO_4$ concentration, due to the increase in ion aggregates at high salt concentration in the organic solvents with low dielectric constants.

The electrochemical stability of various electrolytes was examined by linear sweep voltammetry, and the resulting linear sweep voltammograms are depicted in Figure 3. In the cathodic scan, all the electrolytes showed a large reductive current around 0 V vs. Na/Na^+, corresponding to the reductive deposition of sodium ($Na^+ + e \rightarrow Na$) onto the electrode. No significant reductive decomposition of the electrolyte could be observed prior to the sodium deposition. With respect to anodic stability, the oxidative current started to gradually increase at low potential (around 3.5 V vs. Na/Na^+) in the DME electrolyte, which can be attributed to the oxidative decomposition of the

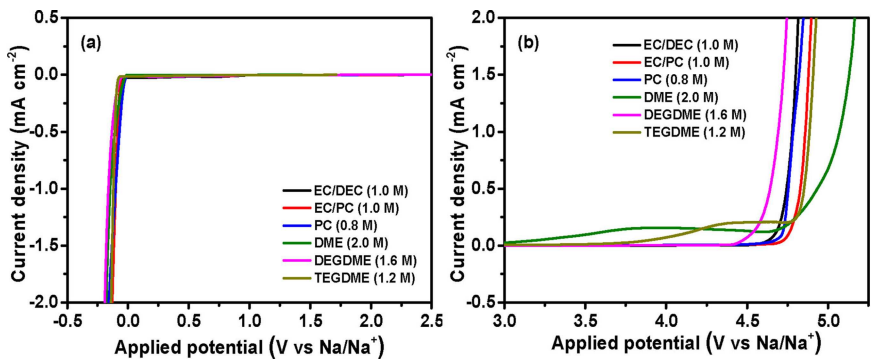

Figure 3. Linear sweep voltammograms of different liquid electrolytes: a) cathodic scan and b) anodic scan (scan rate: 1.0 mV s^{-1}, temperature: 25 °C).

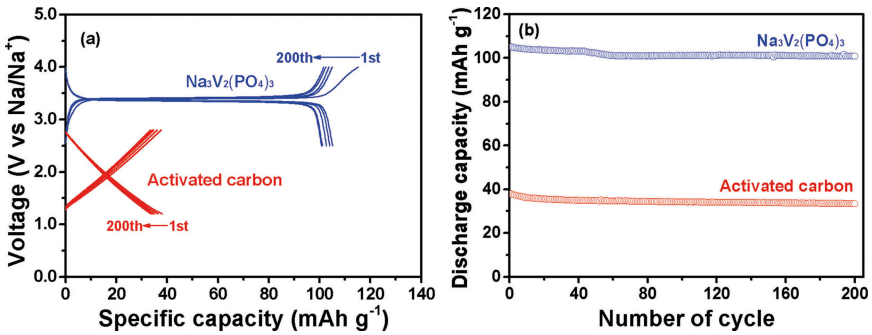

Figure 4. a) Charge and discharge curves of the activated carbon and $Na_3V_2(PO_4)_3$ electrodes employing 1.0 M $NaClO_4$-EC/PC electrolyte, and b) their discharge capacities as a function of the cycle number (current rate: 25 mA g^{-1}, temperature: 25 °C).

electrolyte. In case of the TEGDME and DEGDME electrolytes, the anodic stability was limited to about 4.0 and 4.4 V vs. Na/Na^+, respectively. In contrast, the EC/DEC and PC electrolytes exhibited oxidative stability higher than 4.6 V, and the EC/PC electrolyte showed the highest anodic stability among the electrolytes investigated. These results indicate that the oxidative stability of carbonate-based electrolytes is superior to that of ether-based electrolytes.

Carbon-coated NVP was synthesized, and its morphology was characterized using SEM and TEM. As presented in previous work,[5b] the particles were spherical with an average size of 2 μm, and a carbon layer with a thickness of 5 nm was uniformly coated on the surface of the NVP particles, which could enhance the electronic conductivity of the active materials. Cycling performance of the AC and NVP electrodes assembled with 1.0 M $NaClO_4$-EC/PC electrolyte was evaluated at a constant current rate of 25 mA g^{-1}. Figure 4a presents the voltage profiles of the AC and NVP electrodes with repeated cycling. The charge and discharge curves of the NVP electrode showed a plateau around 3.4 V vs. Na/Na^+, which can be attributed to the reversible phase transformation between $NaV_2(PO_4)_3$ and $Na_3V_2(PO_4)_3$ due to the V_3^+/V_4^+ or V_4^+/V_3^+ redox reactions.[11] The voltage profiles of the AC electrode exhibited a linear charge and discharge behavior, indicating that charge storage mainly occurred by a surface adsorption/desorption of ions on the surface of activated carbon.[12] As shown in Figure 4b, the NVP electrode delivered stable discharge capacities around 105.0 mAh g^{-1} based on the active NVP material. The highly stable cycling behavior of the NVP electrode results from the highly reversible intercalation and deintercalation of Na^+ ions in the structure of NVP without irreversible decomposition of the electrolyte. The AC electrode delivered discharge capacities around 36.0 mAh g^{-1} with excellent cycling stability, indicating that the adsorption and desorption process of ions without any faradaic reactions is highly reversible.

To compare the oxidative stability of the optimized electrolytes under high voltage conditions at the NVP positive electrode, the leakage currents of the Na/NVP cells employing different electrolytes were monitored over time at a constant voltage of 4.0 V. Figure 5 shows the variation in current of the Na/NVP cells as a function of time. It is well known that the current generated at high voltage is influenced by oxidative

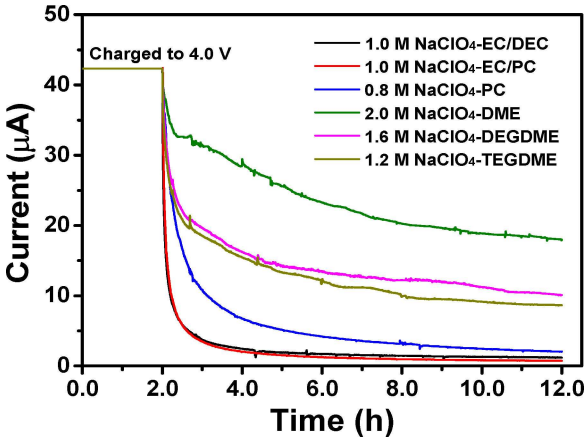

Figure 5. Current variation of Na/$Na_3V_2(PO_4)_3$ cells maintained at a charged voltage of 4.0 V for 10 h at 25 °C.

decomposition of the electrolytes.[13] The cells with ether-based electrolytes showed relatively high current, indicating larger oxidative decomposition of the electrolyte at the NVP electrode. The cell employing 2.0 M $NaClO_4$-DME electrolyte exhibited the highest current. This result was due to the low oxidative stability of the electrolyte, as discussed in Figure 3b. In contrast, the cells with carbonate-based electrolytes showed lower current, indicating better oxidative stability of carbonate-based electrolytes compared to ether-based electrolytes at high voltage, which is consistent with linear sweep voltammetry results.

SICs composed of AC negative electrode and NVP positive electrode were assembled using optimized electrolytes, and their cycling performance was evaluated at a constant current density of 500 mA g^{-1}. The mass ratio of active materials in the negative electrode to the positive electrode has been optimized to 3.2:1.0 to obtain the best cycling performance. Figure 6a and Figure S3 show the charge and discharge curves of SICs assembled with different electrolytes with repeated cycling. The voltage profiles of the SICs are somewhat different from those of an electric double layer capacitor (EDLC) that shows triangularly shaped charge/discharge curves. This result suggests that both non-faradaic surface charge storage in the AC electrode and intercalation/deintercalation of Na ions in the

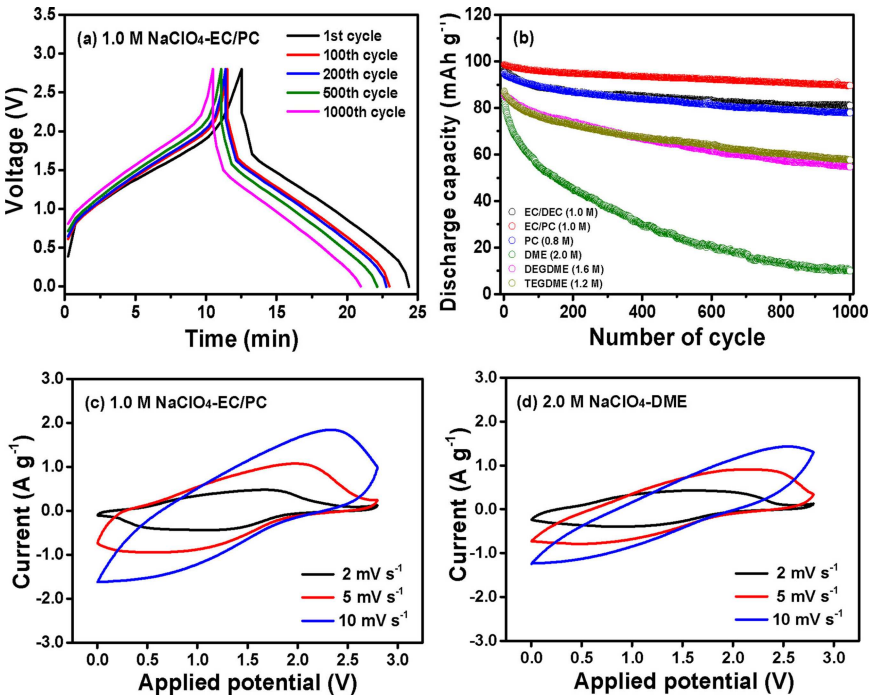

Figure 6. a) Charge and discharge curves of the SIC employing 1.0 M $NaClO_4$-EC/PC at a current density of 500 mA g^{-1}, b) cycling performance of SICs assembled with different liquid electrolytes at a current density of 500 mA g^{-1}, and cyclic voltammograms of SICs with various electrolytes at different scan rates: c) EC/PC and d) DME.

NVP electrode occur simultaneously in this hybrid capacitor. When comparing the initial coulombic efficiencies of the cells, the carbonate-based cells exhibited coulombic efficiencies higher than 94.0% for the first cycle. In contrast, the cells employing ether-based electrolytes showed relatively low initial coulombic efficiencies of 87.1, 88.9 and 89.7% for DME, DEGDME and TEGDME electrolytes, respectively, which can be ascribed to irreversible decomposition of the electrolyte during the first cycle. The cell assembled with 1.0 M $NaClO_4$-EC/PC electrolyte showed stable cycling behavior without a significant increase in overpotential during cycling. Figure 6b shows the discharge capacities of SICs with different electrolytes as a function of cycle number. In this figure, the discharge capacity was calculated based on the mass of active NVP material in the positive electrode. It is clearly seen that the SICs assembled with carbonate-based electrolytes exhibited higher discharge capacities and better cycling stability than those employing ether-based electrolytes. Among the cells, the cell with 1.0 M $NaClO_4$-EC/PC electrolyte delivered the highest initial discharge capacity with the best capacity retention of 90.8% after 1000 cycles. Although the DME electrolyte has the highest ionic conductivity at optimized $NaClO_4$ concentration, the cell with DME electrolyte exhibited low discharge capacities with large capacity fading during cycling. The DME-based cell delivered a discharge capacity of 10.0 mAh g^{-1} at 1000th cycle, which corresponded to a capacity retention of 11.8% with respect to its initial discharge capacity. Such a difference in the cycling performance of SICs is related to the electrochemical stability of the electrolyte and charge/discharge kinetics at the electrolyte-electrode interface. To examine the electrochemical behavior of the SICs with different electrolytes, cyclic voltammetry (CV) was performed, and the results are presented in Figure 6c–d and Figure S4. The obtained cyclic voltammograms are asymmetrical due to the combined process of non-faradaic surface charge storage on AC electrode and intercalation/deintercalation of Na ions in the NVP electrode.[5b] The cells with carbonate-based electrolytes showed higher peak currents than those with ether-based electrolytes. Moreover, the potential differences between anodic peaks and cathodic peaks were lower in the cells with carbonate-based electrolytes. These results indicate fast electrochemical reaction kinetics and low overpotential in the cells with carbonate-based electrolytes. Considering the initial coulombic efficiencies of the cells, leakage current behavior and CV results, the cycling characteristics of SICs depend on the electrochemical stability of the electrolyte and the electrochemical reaction kinetics rather than the ionic conductivity of the electrolyte. This is a reason why the SIC employing the highly conductive electrolyte (2.0 M $NaClO_4$-DME) showed the lowest cycling performance. The higher discharge capacity of SICs with carbonate-based electrolytes resulted from the large number of free ions in the electrolytes, the superior electrochemical stability and the favorable electrochemical reaction kinetics. Accordingly, the cell assembled with 1.0 M $NaClO_4$-EC/PC exhibited the best cycling performance in terms of discharge capacity and cycling stability.

The EDLCs composed of symmetric AC electrodes were assembled using optimized electrolytes, and their cycling performance was evaluated at a constant current density of 1.6 A g^{-1} to investigate the effect of organic solvent on the electrochemical behavior of AC electrode. As shown in Fig-

ure S5a, the EDLC assembled with 1.0 M $NaClO_4$-EC/PC showed the triangular voltage profiles, which indicates good capacitive properties for EDLCs. The cycling performance of EDLCs with different electrolytes is compared in Figure S5b. Clearly, the carbonate-based cells exhibited higher specific capacitance and better cycling stability than the ether-based cells. The cell employing 1.0 M $NaClO_4$-EC/PC showed the highest specific capacitance among the cells because of large number of free ions in the electrolyte. In the case of the ether-based cells, the specific capacitance followed the order of DME > DEGDME > TEGDME. The cell with DME electrolyte exhibited the largest capacity fading with cycling due to its narrow electrochemical stability window. These results support that the carbonate-based electrolytes provide good cycling performance in the EDLC as well as SIC.

To gain further insight into the internal resistances of the SICs with different electrolytes, AC impedance of the cells was measured before and after 1000 cycles, and the resulting AC impedance spectra are presented in Figure 7. All the spectra consist of a depressed semicircle in the high to middle frequency range and a capacitive spike in the low frequency region. The high-frequency intercept on the real axis is attributed to the electrolyte resistance (R_e). The depressed semicircle observed in the high to middle frequency region arises from the charge transfer resistance corresponding to the electronic/ionic resistances in the AC electrode ($R_{ct,a}$) and charge transfer reaction at the electrolyte/NVP interface ($R_{ct,c}$).[14] Z_w is the Warburg impedance related to the sodium ion diffusion within the electrode.[6a,14a] These spectra could be fitted by using the equivalent circuit given in the inset of Figure 7a. As presented in Figure 7a, the cells showed a decreasing trend of R_e with increasing ionic conductivity of electrolyte. When comparing the interfacial resistance (R_{int}; sum of $R_{ct,a}$ and $R_{ct,c}$) and the sloping line, the cells with carbonate-based electrolytes exhibited slightly lower R_{int} and steeper slope as compared to the cells employing ether-based electrolytes, indicating the facile electrochemical reaction and faster ion diffusion in the carbonate-based cell. After 1000 cycles, the values of R_{int} in the cells with ether-based electrolytes significantly increased, which was attributed to the formation of a resistive layer on the surface of the electrode due to electrolyte decomposition during repeated cycling. Formation and growth of the resistive layer on the electrode surface may retard the charge transfer reaction in the cell, which results in an increase in R_{int}.[15] Among the cells, the DME-based cell showed the largest increase in R_{int}, which can be ascribed to the significant decomposition of the electrolyte during cycling. In contrast, the increases of R_{int} in the cells with carbonate-based electrolytes were very small, indicating that the carbonate-based electrolytes are very stable and do not undergo irreversible degradation during the repeated charge and discharge cycles.

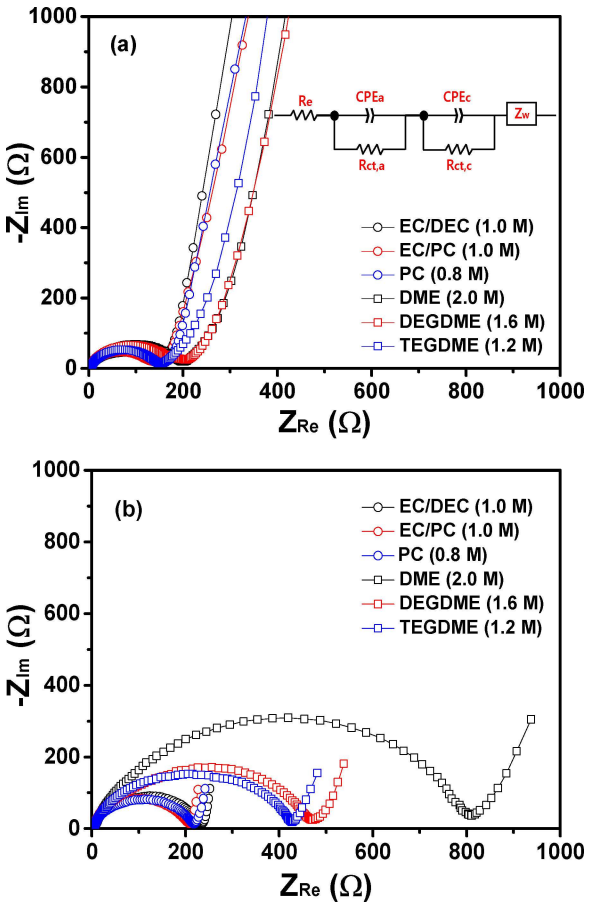

Figure 7. AC impedance spectra of SICs assembled with different liquid electrolytes: a) before cycling and b) after 1000 cycles.

To examine the electrochemical behavior of SICs assembled with different types of electrodes, the different types of SICs (AC negative electrode/$Na_3V_2(PO_4)_2F_3$ positive electrode, $Fe_{1-x}S$@N-doped carbon negative electrode/AC positive electrode) were assembled using optimized electrolytes, and their cycling performance was compared. Figure S6a and S6c show the charge and discharge curves of two different SICs employing 1.0 M $NaClO_4$-EC/PC, and Figure S6b and S6d present the discharge capacities of two SICs with different electrolytes as a function of cycle number. As shown in figure, the cells with carbonate-based electrolytes delivered higher discharge capacities than the cells with ether-based electrolytes. Among them, the cells employing 1.0 M $NaClO_4$-EC/PC showed the highest discharge capacity and stable cycling behavior. These additional results confirm that 1.0 M $NaClO_4$-EC/PC is the most appropriate electrolyte for achieving good electrochemical performance of sodium-ion hybrid capacitors.

Rate capabilities of SICs with different electrolytes were evaluated at various current rates. The cells were charged and discharged at constant current with increasing current density from 20 to 1000 mA g^{-1} every five cycles. Figure 8a shows the charge and discharge curves of the cell with 1.0 M $NaClO_4$-EC/PC electrolyte at different current densities, and Figure 8b compares the rate capability of the cells assembled with different electrolytes. It is clearly seen that the carbonate-based cell delivered higher discharge capacities than the cells with ether-based electrolytes at high current rates. The enhanced rate capability of the carbonate-based cells can be attributed to the facile electrochemical reaction kinetics and the large number of free ions in the electrolyte. The cell with 1.0 M

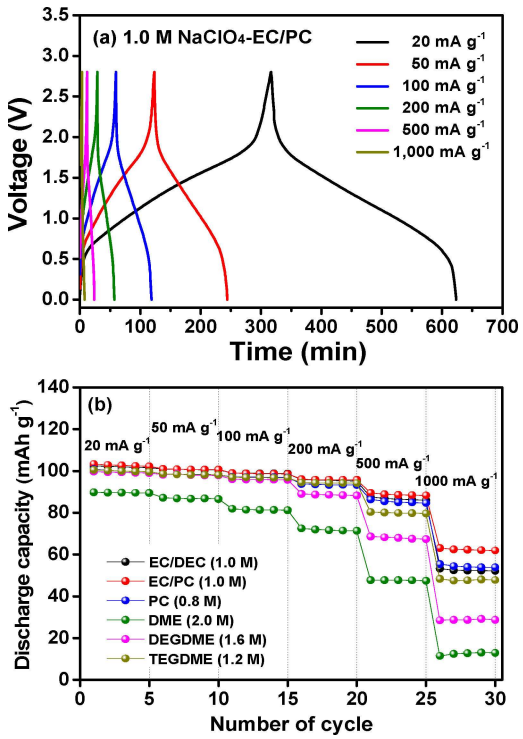

Figure 8. a) Charge and discharge curves of an SIC employing 1.0 M $NaClO_4$-EC/PC at various current densities and b) discharge capacities of SICs with different electrolytes at increasing current density from 20 to 1,000 mA g^{-1}.

$NaClO_4$-EC/PC electrolyte delivered the highest discharge capacity (63.1 mAh g^{-1}) at 1000 mA g^{-1}. Overall, our results demonstrate that 1.0 M $NaClO_4$-EC/PC is the most appropriate electrolyte for achieving good cycling performance of sodium-ion hybrid capacitors in terms of reversible capacity, cycling stability and rate capability.

3. Conclusions

We investigated the effect of organic solvent on the electrochemical performance of sodium-ion hybrid capacitors, and it was demonstrated that the physicochemical properties of organic solvents significantly influenced the electrochemical characteristics of SICs. The most critical properties of the electrolyte that affect the cycling performance of SICs is not ionic conductivity but number of free ions and oxidative stability at high voltage. Thus, the cell assembled with 1.0 M $NaClO_4$-EC/PC exhibited the best cycling performance in terms of discharge capacity, cycling stability and rate capability, which is due to the high concentration of free ions, facile electrochemical reaction kinetics and superior electrochemical stability of the electrolyte.

Experimental Section

Electrolytes

The electrolyte was handled and prepared in a glove box filled with high-purity argon gas. $NaClO_4$ (anhydrous, 99.5%, Alfa Aesar) was used after vacuum drying at 120 °C for 24 h. DEC (anhydrous, ≥99%, Sigma Aldrich), EC (anhydrous, 99.0%, Sigma Aldrich), PC (anhydrous, 99.7%, Sigma Aldrich), DME (anhydrous, 99.5%, Sigma Aldrich), DEGDME (anhydrous, 99.5%, Sigma Aldrich) and TEGDME (>98.0%, TCI) were used as organic solvents. A binary solvent mixture was prepared by mixing two solvents with a volume ratio of 50/50. The electrolytes were dried over molecular sieves to reduce water content. Karl Fisher titration (Mettler-Toledo Coulometer) confirmed that the water content was less than 25 ppm in the electrolytes.

Electrode Preparation and Cell Assembly

AC with a specific surface area of 2200 $m^2 g^{-1}$ was kindly supplied by Power Carbon Technology and used as an active material for negative electrode. Carbon coated-NVP was synthesized by a sol-gel technique, as previously reported[5b] and was used as an active material for the positive electrode. $Na_3V_2(PO_4)_2F_3$ and $Fe_{1-x}S$@N-doped carbon were synthesized, as reported earlier.[16] The electrodes were prepared by coating an N-methyl-2-pyrrolidone (NMP)-based slurry containing 80 wt.% active material, 10 wt.% Ketjen black and 10 wt.% poly(vinylidene fluoride) binder onto an aluminum foil. The resulting electrodes were dried in a vacuum oven at 110 °C for 12 h. The active mass loadings of AC and NVP in the electrodes were about 5.1 and 1.6 mg cm^{-2}, respectively. The sodium-ion hybrid capacitor was assembled by sandwiching a glass fiber separator (ADVANTEC, GC-50) between two electrodes. It was then enclosed in a CR2032-type coin cell and injected with different types of liquid electrolytes. All cells were assembled in a glove box filled with high purity Ar gas.

Characterization and Measurements

The ionic conductivity and viscosity of the electrolytes were measured using a Cond 3210 conductivity meter (WTW GmbH, Germany) and a viscometer (microVISC, Rheosense, USA) at 25 °C, respectively. Linear sweep voltammetry (LSV) was conducted at a scan rate of 1.0 mV s^{-1} to evaluate the electrochemical stability of the electrolyte on a platinum working electrode with sodium metal as reference and counter electrodes. Attenuated total reflectance Fourier transform infrared (ATR-FTIR) spectra were recorded in the range of 400–4000 cm^{-1} using a Nicolet iS50 spectrometer. Cyclic voltammetry was performed using a Zahner Electrik IM6 over a potential range of 0 to 2.8 V with various scan rates at 25 °C. Charge and discharge cycling tests of the SICs were conducted at constant current densities in the voltage range of 0.0–2.8 V at 25 °C using battery test equipment (WBCS 3000, Wonatech). Cycling tests of half-cells (Na/activated carbon, $Na/Na_3V_2(PO_4)_3$) were conducted in the voltage ranges of 1.2–2.8 V for activated carbon electrode and 2.5–4.0 V for $Na_3V_2(PO_4)_3$ electrode with Na metal as a reference electrode. Cycling tests of the EDLCs were performed in the voltage range of 0.0–2.8 V at 25 °C. Specific capacitance of the EDLCs was calculated from the cycling data, as reported earlier.[17] Electrochemical impedance spectroscopy (EIS) of SICs was carried out using a Zahner Elektrik IM6 impedance analyzer over a frequency range of 5 mHz to 100 kHz with an amplitude of 5 mV.

Acknowledgements

This work was supported by the National Research Foundation of Korea (NRF) grant funded by the Korea government (Ministry of Science, ICT & Future Planning) (No. 2016R1A4A1012224) and the Industrial Promotion Program of Economic Cooperation Area of MOTIE/KIAT [R0004005].

Conflict of Interest

The authors declare no conflict of interest.

Keywords: electrochemical performance · energy storage · liquid electrolyte · organic solvent · sodium-ion hybrid capacitor

[1] a) J. M. Tarascon, M. Armand, *Nature* **2001**, *414*, 359–367; b) M. Armand, J. M. Tarascon, *Nature* **2008**, *451*, 652–657; c) V. Etacheri, R. Marom, R. Elazari, G. Salitra, D. Aurbach, *Energy Environ. Sci.* **2011**, *4*, 3243–3262; d) B. Dunn, H. Kamath, J. M. Tarascon, *Science* **2011**, *334*, 928–935.

[2] a) H. Kawamoto, W. Tamaki, *Sci. Technol. Trends, Quart. Rev.* **2011**, *39*, 51; b) N. Yabuuchi, K. Kubota, M. Dahbi, S. Komaba, *Chem. Rev.* **2014**, *114*, 11636–11682; c) M. D. Slater, D. Kim, E. Lee, C. S. Johnson, *Adv. Funct. Mater.* **2013**, *23*, 947–958.

[3] a) Y. Lee, J. Lee, H. Kim, K. Kang, N.-S. Choi, *J. Power Sources* **2016**, *320*, 49–58; b) R. Thangavel, B. Moorthy, D. K. Kim, Y.-S. Lee, *Adv. Energy Mater.* **2017**, *7*, 1602654.

[4] S. Y. Hong, Y. Kim, Y. Park, A. Choi, N.-S. Choi, K. T. Lee, *Energy Environ. Sci.* **2013**, *6*, 2067–2081.

[5] a) E. Lim, C. Jo, M. S. Kim, M.-H. Kim, J. Chun, H. Kim, J. Park, K. C. Roh, K. Kang, S. Yoon, J. Lee, *Adv. Funct. Mater.* **2016**, *26*, 3711–3719; b) R. Thangavel, K. Kaliyappan, K. Kang, X. Sun, Y.-S. Lee, *Adv. Energy Mater.* **2016**, *6*, 1502199; c) H. Li, L. Peng, Y. Zhu, X. Zhang, G. Yu, *Nano Lett.* **2016**, *16*, 5938–5943.

[6] a) F. Yao, D. T. Pham, Y. H. Lee, *ChemSusChem* **2015**, *8*, 2284–2311; b) D. P. Dubal, O. Ayyad, V. Ruiz, P. Gomez-Romero, *Chem. Soc. Rev.* **2015**, *44*, 1777–1790.

[7] a) H.-K. Roh, M.-S. Kim, K. Y. Chung, M. Ulaganathan, V. Aravindan, S. Madhavi, K. C. Roh, K.-B. Kim, *J. Mater. Chem. A* **2017**, *5*, 17506–17516; b) B. Babu, M. M. Shaijumon, *J. Power Sources* **2017**, *353*, 85–94; c) X. Wang, S. Kajiyama, H. Iinuma, E. Hosono, S. Oro, I. Moriguchi, M. Okubo, A. Yamada, *Nat. Commun.* **2015**, *6*, 6544.

[8] a) A. Ponrouch, D. Monti, A. Boschin, B. Steen, P. Johansson, M. R. Palacin, *J. Mater. Chem. A* **2015**, *3*, 22–42; b) H. Che, S. Chen, Y. Xie, H. Wang, K. Amine, X.-Z. Liao, Z.-F. Ma, *Energy Environ. Sci.* **2017**, *10*, 1075–1101; c) A. Ponrouch, R. Dedryvere, D. Monti, A. E. Demet, J. M. Ateba Mba, L. Croguennec, C. Masquelier, P. Johansson, M. R. Palacín, *Energy Environ. Sci.* **2013**, *6*, 2361–2369; d) P. K. Dutta, S. Mitra, *J. Power Sources* **2017**, *349*, 152–162; e) A. Eftekhari, D.-W. Kim, *J. Power Sources* **2018**, *395*, 336–348.

[9] a) K. Saravanan, C. W. Mason, A. Rudola, K. H. Wong, P. Balaya, *Adv. Energy Mater.* **2013**, *3*, 444–450; b) S. Y. Lim, H. Kim, R. A. Shakoor, Y. Jung, J. W. Choi, *J. Electrochem. Soc.* **2012**, *159*, A1393-A1397.

[10] a) C. K. Lin, I. D. Wu, *Polymer* **2011**, *52*, 4106–4113; b) W. Wieczorek, P. Lipka, G. Zukowska, H. Wycislik, *J. Phys. Chem. B* **1998**, *102*, 6968–6974.

[11] a) Y. H. Jung, C. H. Lim, D. K. Kim, *J. Mater. Chem. A* **2013**, *1*, 11350–11354; b) X. Rui, W. Sun, C. Wu, Y. Yu, Q. Yan, *Adv. Mater.* **2015**, *27*, 6670–6676.

[12] A. G. Kannan, A. Samuthirapandian, D.-W. Kim, *J. Power Sources* **2017**, *337*, 65–72.

[13] a) Y.-M. Song, C.-K. Kim, K.-E. Kim, S. Y. Hong, N.-S. Choi, *J. Power Sources* **2016**, *302*, 22–30; b) Z. Zhang, L. Hu, H. Wu, W. Weng, M. Koh, P. C. Redfern, L. A. Curtiss, K. Amine, *Energy Environ. Sci.* **2013**, *6*, 1806–1810.

[14] a) S. S. Zhang, K. Xu, T. R. Jow, *Electrochim. Acta* **2006**, *51*, 1636–1640; b) C. Lei, F. Markoulidis, Z. Ashitaka, C. Lekakou, *Electrochim. Acta* **2013**, *92*, 183–187.

[15] a) J.-H. Kim, H.-S. Woo, W. K. Kim, K. H. Ryu, D.-W. Kim, *ACS Appl. Mater. Interfaces* **2016**, *8*, 32300–32306; b) S.-R. Park, Y.-C. Jung, W.-K. Shin, K. H. Ahn, C. H. Lee, D.-W. Kim, *J. Membr. Sci.* **2017**, *527*, 129–136.

[16] a) Q. Liu, D. Wang, X. Yang, N. Chen, C. Wang, X. Bie, Y. Wei, G. Chen, F. Du, *J. Mater. Chem. A* **2015**, *3*, 21478–21485; b) G. K. Veerasubramani, Y. Subramanian, M.-S. Park, G. Nagaraju, B. Senthilkumar, Y.-S. Lee, D.-W. Kim, *J. Mater. Chem. A* **2018**, *6*, 20056–20068.

[17] R. Thangavel, A. G. Kannan, R. Ponraj, V. Thangavel, D.-W. Kim, Y.-S. Lee, *J. Power Sources* **2018**, *383*, 102–109.

Manuscript received: October 26, 2018
Revised manuscript received: November 30, 2018
Accepted manuscript online: November 30, 2018
Version of record online: December 19, 2018